An Iron Polyolate Complex as a Precursor for the Controlled Synthesis of Monodispersed Iron Oxide Colloids

Markus Niederberger,[†] Frank Krumeich,[†] Kaspar Hegetschweiler,[‡] and Reinhard Nesper*,[†]

Laboratory of Inorganic Chemistry, Swiss Federal Institute of Technology (ETH), Hönggerberg HCI H139, CH-8093 Zürich, Switzerland, and Institute of Inorganic Chemistry, University of Saarland, Postfach 15 11 50, D-66041 Saarbrücken, Germany

A simple procedure that applies a hexanuclear iron–polyolate complex as an iron oxide precursor has been developed for the synthesis of colloidal iron oxide particles. The hydrolysis of this complex and the subsequent hydrothermal treatment of the intermediate product yield monodispersed hematite particles with a disclike shape. The outer diameter is about 1 μm and the thickness about 250 nm. The particles consist of small platelike crystallites that are almost perfectly aligned in the *a–b* plane. If acetyl acetone is added during the synthesis, similar but smaller disclike hematite particles (diameter ∼ 0.25–0.45 μm, thickness ∼ 80 nm) have been obtained. On the other hand, hydrazine as an additive leads to single crystals of hematite in the form of hexagonal platelets (diameter ∼ 0.6–1 μm, thickness ∼ 50 nm).

Introduction

Aiming at novel advanced materials,[1] much effort has been focused on the development of new strategies for the synthesis of monodispersed particles, with sizes typically in the region of a few hundred nanometers to some micrometers.[2,3] The interest in these objects is due to the knowledge that the relevant physical, chemical, and catalytic properties of particles in this size regime depend not only on the chemical composition but crucially also on their size and shape.[4] Thus, a carefully directed improvement of the material properties, especially with regard to specific applications, has to be combined with a tailoring of the particles' chemical, structural, and morphological characteristics. In particular, the required narrow size distribution as well as the homogeneity regarding the particle shape and composition represent the main goal of preparative approaches and can only be achieved by appropriate adjustment of all synthesis parameters.

Although many techniques for the preparation of monodispersed metal (hydrous) oxide colloids have been reported,[2,5–7] it is still rather difficult to produce them in large quantities because the chemical composition and the morphology of the obtained particles strongly depend on a large number of synthesis parameters such as pH, concentration of the reactants, temperature, method of mixing, and rate of oxidation.[2,8] Especially the nature and concentration of anions such as chloride, phosphate, or sulfate have a strong influence on particle size and shape.[9,10] Thus, the sensitivity of the preparation complicates both the reproducibility and the scale-up of the synthesis.

Submicrometric iron oxides[11] are important materials for magnetic,[12,13] catalytic,[14] and pigment applications.[15] In the solution-based synthesis of iron oxide colloids and nanoparticles, several techniques such as sol–gel processes (respectively gel–sol processes),[16,17] forced hydrolysis,[8,18–21] hydrothermal synthesis,[22–25] electro-

(1) Interrante, L. V.; Hampden-Smith, M. J. *Chemistry of Advanced Materials, An Overview*; Wiley–VCH: New York, 1998.

(2) Matijevic, E. *Chem. Mater.* **1993,** *5,* 412.

(3) Fendler, J. H. *Chem. Mater.* **1996,** *8,* 1616.

(4) Suryanarayana, C.; Koch, C. C. *Non-Equilibrium Processing of Materials*; Pergamon Materials Series; Pergamon Press: New York, 1999.

(5) Matijevic, E. *Annu. Rev. Mater. Sci.* **1985,** *15,* 483.

(6) Matijevic, E. *Langmuir* **1986,** *2,* 12.

(7) Matijevic, E. *Langmuir* **1994,** *10,* 8.

(8) Domingo, C.; Rodriguez-Clemente, R.; Blesa, M. *J. Colloid Interface Sci.* **1994,** *165,* 244.

(9) Reeves, N. J.; Mann, S. *J. Chem. Soc., Faraday Trans.* **1991,** *87,* 3875.

(10) Livage, J.; Henry, M.; Sanchez, C. *Prog. Solid State Chem.* **1988,** *18,* 259.

(11) Cornell, R. M.; Schwertmann, U. *The Iron Oxides—Structure, Properties, Reactions, Occurrence and Uses*; VCH Verlagsgesellschaft: Weinheim, 1996.

(12) Kim, D. K.; Zhang, Y.; Voit, W.; Kao, K. V.; Kehr, J.; Bjelke, B.; Muhammed, M. *Scr. Mater.* **2001,** *44,* 1713.

(13) Leslie-Pelecky, D. L.; Rieke, R. D. *Chem. Mater.* **1996,** *8,* 1770.

(14) Rühle, T.; Timpe, O.; Pfänder, N.; Schlögl, R. *Angew. Chem., Int. Ed.* **2000,** *39,* 4379.

(15) Feldmann, C. *Adv. Mater.* **2001,** *13,* 1301.

(16) Sugimoto, T.; Sakata, K. *J. Colloid Interface Sci.* **1992,** *152,* 587.

(17) Sugimoto, T.; Sakata, K.; Muramatsu, A. *J. Colloid Interface Sci.* **1993,** *159,* 372.

(18) Ozaki, M.; Kratohvil, S.; Matijevic, E. *J. Colloid Interface Sci.* **1984,** *102,* 146.

(19) Blesa, M. A.; Matijevic, E. *Adv. Colloid Interface Sci.* **1989,** *29,* 173.

chemical preparation methods,[26] microwave heating,[27] and deposition of organometallic compounds in mesoporous alumina[28] have been reported.

Here, we present a versatile method to synthesize large quantities of monodispersed iron oxide colloids. In contrast to the above-mentioned methods starting from iron salt solutions, we investigated the hydrolysis of the iron–polyolate complex $[N(CH_3)_4]_2[OFe_6-(H_{-3}thme)_3(OCH_3)_3Cl_6]\cdot MeOH$ (thme = 1,1,1-tris(hydroxymethyl)ethane) in the following designated as *Fe₆-complex*, which can easily be prepared in a one-pot synthesis.[29]

Experimental Section

Materials. All chemicals were obtained from Fluka, Switzerland, and used without further purification. $[N(CH_3)_4]_2-[OFe_6(H_{-3}thme)_3(OCH_3)_3Cl_6]\cdot MeOH$ (*Fe₆-complex*) was synthesized according to a previously reported method.[29]

Synthesis. *Without Any Additives.* In a typical procedure, 1.5 g (1.3 Mmol) *Fe₆-complex* is suspended in 4 mL of distilled water, followed by the addition of 3 mL of 1 M NaOH. After being stirred for several minutes, the black solution is mixed with 3 mL of 1 M HCl. The brown suspension ages at room temperature for 24 h under stirring. The hydrothermal treatment in an autoclave (Parr Acid Digestion Bombs with 23-mL Teflon cups) for 1 day at 80 °C and 3 days at 150 °C results in a red product. It is filtered off and washed with ethanol and diethyl ether. For the analysis, the powder is dried in a furnace at 300 °C for 5 h. According to elemental analysis, the amount of organic residues is <1%. To investigate the influence of temperature and duration of hydrothermal treatment, respectively, further experiments under similar conditions were carried out at either 100, 120, 150, or 180 °C and for either 24 h, 48 h, or 7 days at 150 °C.

With Additives. *Fe₆-complex* (1.5 g, 1.3 Mmol) is suspended in 4 mL of distilled water, followed by the addition of 3 mL of 1 M NaOH. The resulting black solution is either mixed with 8 Mmol hydrazine or 1.3 Mmol acetyl acetone, followed by the addition of 3 mL of 1 M HCl. Aging is similar to the standard procedure without any additives. The products are filtered, washed with ethanol and diethyl ether, and finally air-dried.

Characterization. The X-ray powder diffraction (XRD) patterns of all samples were measured in reflection mode (Cu Kα radiation, Ge monochromator) on a Bruker D8 diffractometer equipped with a scintillation counter and a secondary monochromator to suppress fluorescence radiation. Transmission electron microscopy (TEM) investigations were performed on a CM30 ST microscope (Philips), operated at 300 kV. For this, the material was deposited onto a perforated carbon foil supported on a copper grid. Scanning electron microscopy (SEM) was performed on a LEO 1530 microscope, equipped with a field emission gun. Secondary electron images were recorded at low voltage (2 kV), which allows for an observation

of the as-synthesized, uncoated sample without charging problems. Nitrogen adsorption measurements were performed on a Micromeritics ASAP 2010 at 77.35 K. Prior to the measurement, the sample was degassed at 300 °C for 10 h under vacuum. For the determination of the surface area, the BET method with N_2 as the adsorbate was used. C, H, and Cl analysis was carried out by means of combustion test methods on a LECO CHN-900. The iron analysis was performed by inductively coupled plasma/optical emission spectroscopy (ICP–OES) on a Thermo Jarrell Ash IRIS. Magnetic susceptibilities were measured on a squid magnetometer (MPMS 5S, Quantum Design). The quartz sample holder, containing about 20 mg of substance, was rotated by 360° during the measurements. Data were collected from room temperature down to 1.7 K and from −50 to 50 kG.

Results and Discussion

The air-stable iron–polyolate complex $[N(CH_3)_4]_2-[OFe_6(H_{-3}thme)_3(OCH_3)_3Cl_6]\cdot MeOH$ (*Fe₆-complex*) was successfully tested as a new precursor material for the synthesis of iron oxide colloids. Gram quantities of disclike hematite particles with a narrow size distribution can be obtained by a reproducible procedure involving the hydrolysis of the *Fe₆-complex* and subsequent hydrothermal treatment. Similar products with bright red color are formed at temperatures $T \geq 100$ °C. TEM images of the colloids synthesized at 100 °C and at 180 °C are shown in Figures 1a and 1b. Already at 100 °C (Figure 1a), the particles display a smoothly round shape but with sizes varying in a rather wide range (diameter 0.5–1.3 μm). Tilting experiments and particles that lie on the side by chance give clear evidence that the morphology is disklike instead of spherical. After heating at 180 °C, the particle shape and size is still the same but every single particle starts to separate in much smaller, loosely agglomerated subunits (Figure 1b). In contrast to that, the application of a lower temperature (80 °C for 24 h) leads to a brown powder that shows no uniform particle morphology (images not shown here). Interestingly, the disclike particle morphology is already well developed after 24 h at 150 °C (Figure 1c).

The standard procedure without any additives including a hydrothermal treatment at 150 °C for 3 days results in a bright red powder. Figure 2a shows a representative SEM micrograph of this material. The overview image reveals that there are particles of a disc-type shape that have a narrow size distribution, with an average diameter of about 1 μm (0.93 ± 0.2 μm). The product almost exclusively comprises these monodispersed iron oxide colloids. It is interesting to note that compared to the sample obtained after only 24 h at 150 °C that shows varying particle sizes between 0.5 and 1 μm, all particles are practically monodispersed after the 3-days treatment.

SEM images recorded at higher magnification demonstrate several interesting features. Some particles are grown together and interpenetrate each other mutually (Figures 2b,c). Interestingly, this intergrowth does not influence the size and shape of the individual particles. The thickness of one particle is ≈250 nm. A side view on several particles (Figure 2c) reveals a layered structure consisting of much smaller stacked discs. Each of the larger particles is made up of 10–20 agglomerated discs that are about 7–10-nm thick. Figure 2d shows a close view from above on one particle. The crystallites

(20) Ozaki, M.; Ookoshi, N.; Matijevic, E. *J. Colloid Interface Sci.* **1990**, *137*, 546.
(21) Feldmann, C.; Jungk, H.-O. *Angew. Chem., Int. Ed.* **2001**, *40*, 359.
(22) Yitai, Q.; Yi, X.; Chuan, H.; Jing, L.; Zuyao, C. *Mater. Res. Bull.* **1994**, *29*, 953.
(23) Sahu, K. K.; Rath, C.; Mishra, N. C.; Anand, S.; Das, R. P. *J. Colloid Interface Sci.* **1997**, *185*, 402.
(24) Li, Y.; Liao, H.; Qian, Y. *Mater. Res. Bull.* **1998**, *33*, 841.
(25) Chen, D.; Xu, R. *J. Solid State Chem.* **1998**, *137*, 185.
(26) Pascal, C.; Pascal, J. L.; Favier, F.; Moubtassim, M. L. E.; Payen, C. *Chem. Mater.* **1999**, *11*, 141.
(27) Palchik, O.; Felner, I.; Kataby, G.; Gedanken, A. *J. Mater. Res.* **2000**, *15*, 2176.
(28) Schneider, J. J.; Czap, N.; Hagen, J.; Engstler, J.; Ensling, J.; Gütlich, P.; Reinoehl, U.; Bertagnolli, H.; Luis, F.; Jos de Jongh, L.; Wark, M.; Grubert, G.; Hornyak, G. L.; Zanoni, R. *Chem. Eur. J.* **2000**, *6*, 4305.
(29) Cornia, A.; Gatteschi, D.; Hegetschweiler, K.; Hausherr-Primo, L.; Gramlich, V. *Inorg. Chem.* **1996**, *35*, 4414.
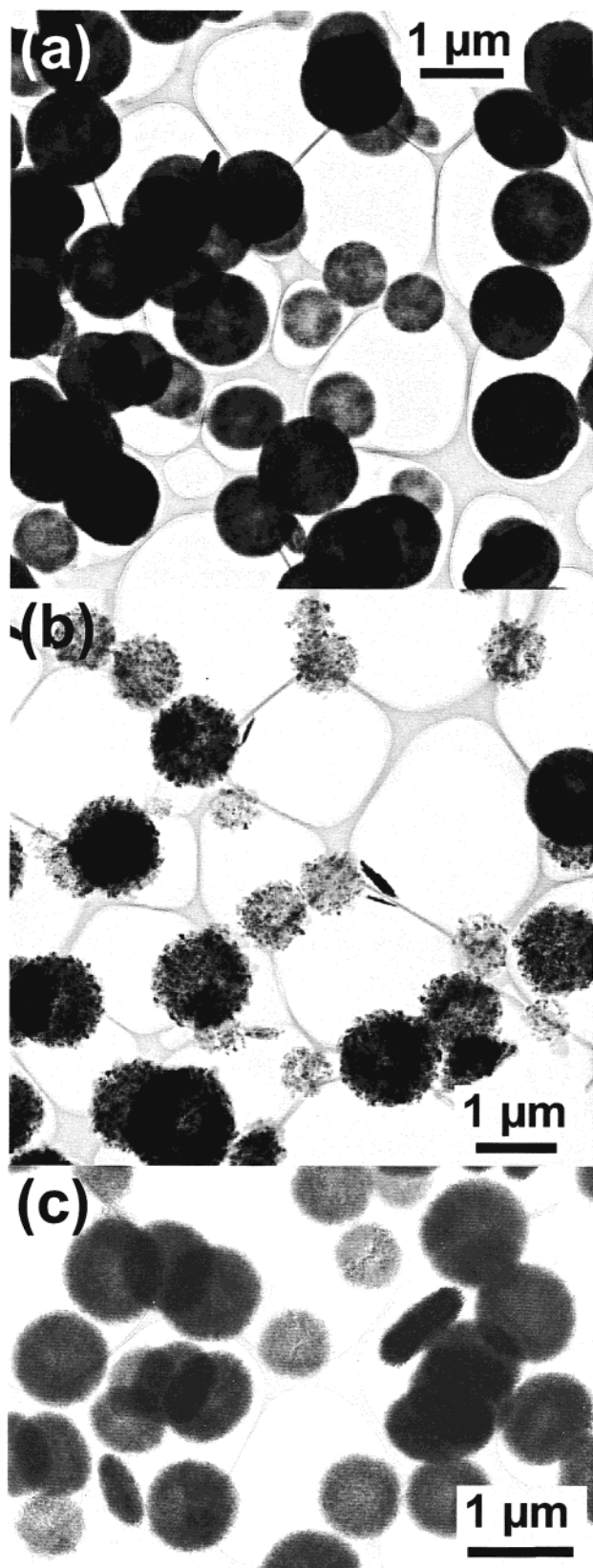
Figure 1. TEM images of the product obtained from hydrolysis of the *Fe6-complex* and hydrothermal treatment at (a) 100 °C for 3 days, (b) 180 °C for 3 days, and (c) 150 °C for 24 h.

of one layer seem to be grown from inside to outside; however, they may be secondary aggregates that form after a primary nucleation process as well. The rough surface clearly gives evidence that the particles are polycrystals.
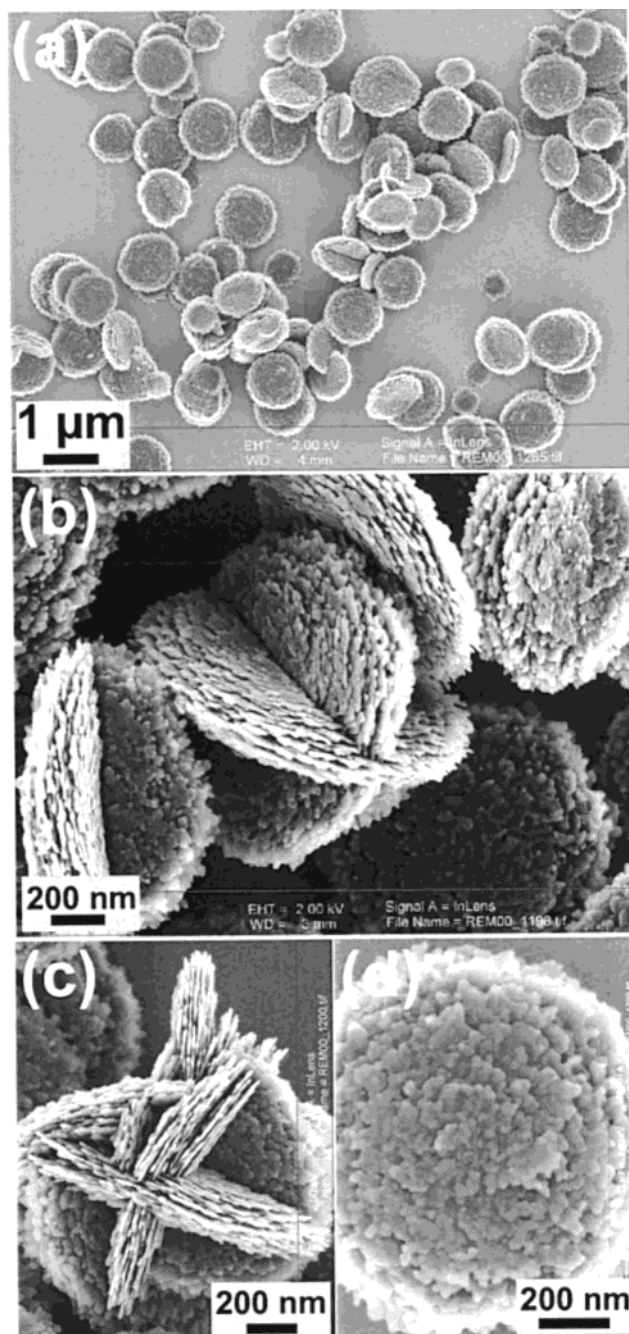

Figure 2. Representative SEM images of the final material obtained from the *Fe6-complex* after hydrolysis and hydrothermal treatment at 150 °C for 3 days. (a) Survey. (b)−(d) Higher magnified images. The particles are sometimes intergrown (b, c). A side view of an agglomeration of particles reveals the layered structure (c). The top view on a single particle shows that small crystallites built up the layers (d).

The X-ray powder pattern (Figure 3) matches that of hematite α-Fe_2O_3. The reflections are indexed accordingly. Interestingly, the reflections indexed with 110, 300, and 220 are much sharper than the other peaks; that is, the reflections *hkl* with $l = 0$ are sharp, whereas the reflections *hkl* with $l \neq 0$ are broad. This observation is reasonable considering the structure of the particles that are iron oxide platelets stacked along the *c* axis (cf. Figure 2c). The relatively sharp reflections *hk*0 are an indication of the well-ordered orientation of all platelets in each of the larger particles. On the other hand, misalignments between the plane normals of the
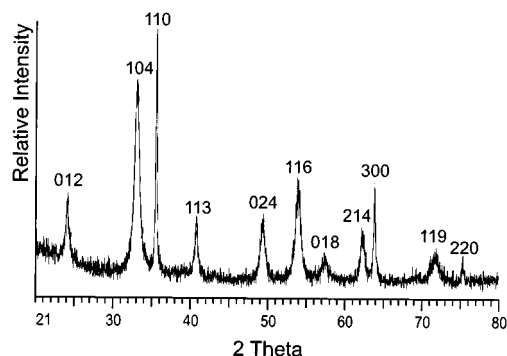
Figure 3. XRD pattern of the hematite particles obtained from hydrolysis of the *Fe$_6$-complex* and hydrothermal treatment at 150 °C for 3 days. The reflections *hkl* with $l = 0$ are sharper than the ones with $l \neq 0$.
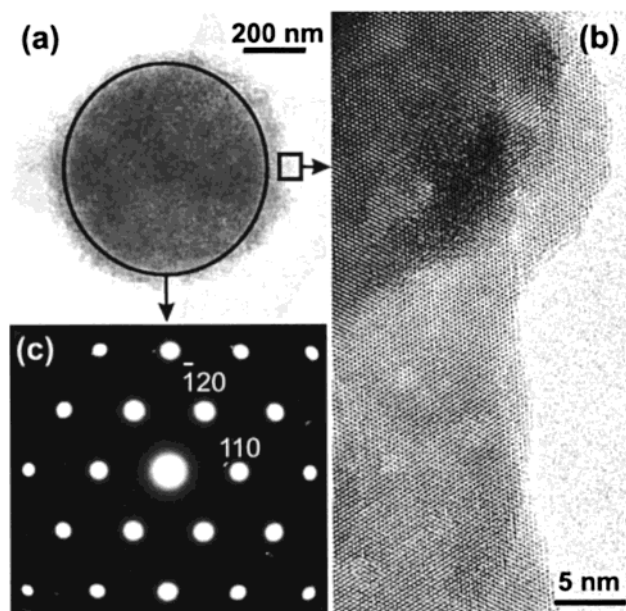

Figure 4. Hematite particles obtained from hydrolysis of the *Fe$_6$-complex* and hydrothermal treatment at 150 °C for 3 days. (a) TEM image of a single particle. (b) HRTEM image of a part of such an iron oxide particle showing the crystal structure as a hexagonal pattern of dark dots. (c) Typical selected area electron diffraction pattern of an iron oxide particle along the *c* axis. The hexagonal arrangement of spots *hk*0 corresponds to a hexagonal lattice with $a = 5.04$ Å.

different platelets in the stacking direction occur, inducing disorder. Therefore, the reflections *hkl* ($l \neq 0$) are broader.

An electron diffraction pattern and high-resolution TEM micrograph recorded from one individual particle are presented in Figure 4. The HRTEM image (Figure 4b) clearly demonstrates the internal composite nature of the particles. Small single crystallites with diameters ranging from 50 to 150 nm are perfectly aligned, and a hexagonal pattern of dark dots can be seen in the whole region. Selected area electron diffraction performed on the whole particle surprisingly shows that this mosaic structure indeed behaves similar to a single crystal, giving a spot pattern (Figure 4c) characteristic of the hexagonal lattice of hematite ($a = 5.04$ Å). These observations confirm that the disclike particles consist of small single crystals in a perfectly aligned manner and that the particle resultantly appears as a quasi-single crystal. However, small bright patches in the
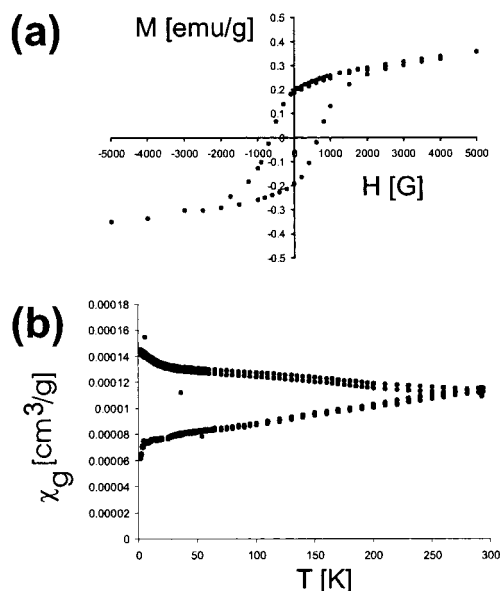

Figure 5. Magnetic investigations of the hematite particles obtained from hydrolysis of the *Fe$_6$-complex* and hydrothermal treatment at 150 °C for 3 days. (a) Hysteresis loop at 293 K in a plot of magnetization versus applied magnetic field. (b) ZFC and FC magnetization as a function of temperature for the calcined iron oxide platelets at an applied field of 100 G.

HRTEM images of the platelets (Figure 4b) may hint at pores perpendicular to the *c* axis. Besides that, the SEM images demonstrate the presence of cavities between the small platelike crystals. Considering these results, the surface area of 51 m^2/g (BET measurement) seems to be rather small.

The field-dependent magnetization curve of the material shows a hysteresis with a remanent magnetization of about 0.19 emu/g at zero field and a coercivity of 55.6 A/m (Figure 5a). This is comparable to the magnetic properties of other nanoparticular hematite samples.[28] The temperature-dependent magnetization curves cooled in the absence (zero-field-cooled, ZFC) or presence (field-cooled, FC) of a magnetic field are shown in Figure 5b. The ZFC branch exhibits a steadily increasing susceptibility with rising temperature with a practically linear characteristic and, thus, no indication for a blocking temperature up to 300 K. The subsequent cooling in the presence of the magnetic field of 100 G further enhances the magnetization with decreasing temperature. This property is known to be due to a freezing of the magnetic domains oriented parallel to the magnetic field. From both field and temperature dependence we conjecture that the small nano discs are magnetically coupled up to room temperature and consequently that the large platelets act as magnetically more or less homogeneous particles in the investigated temperature and field ranges.

In an approach similar to the work of Sapieszko and Matijevic,[30] the influence of the redox-active agent hydrazine on the oxidation state of the final products was investigated. TEM micrographs (Figure 6a) clearly reveal a different particle geometry: the platelike iron oxide crystals exhibit a hexagonal shape. The platelets have diameters ranging from about 0.6 to 1 μm, with a

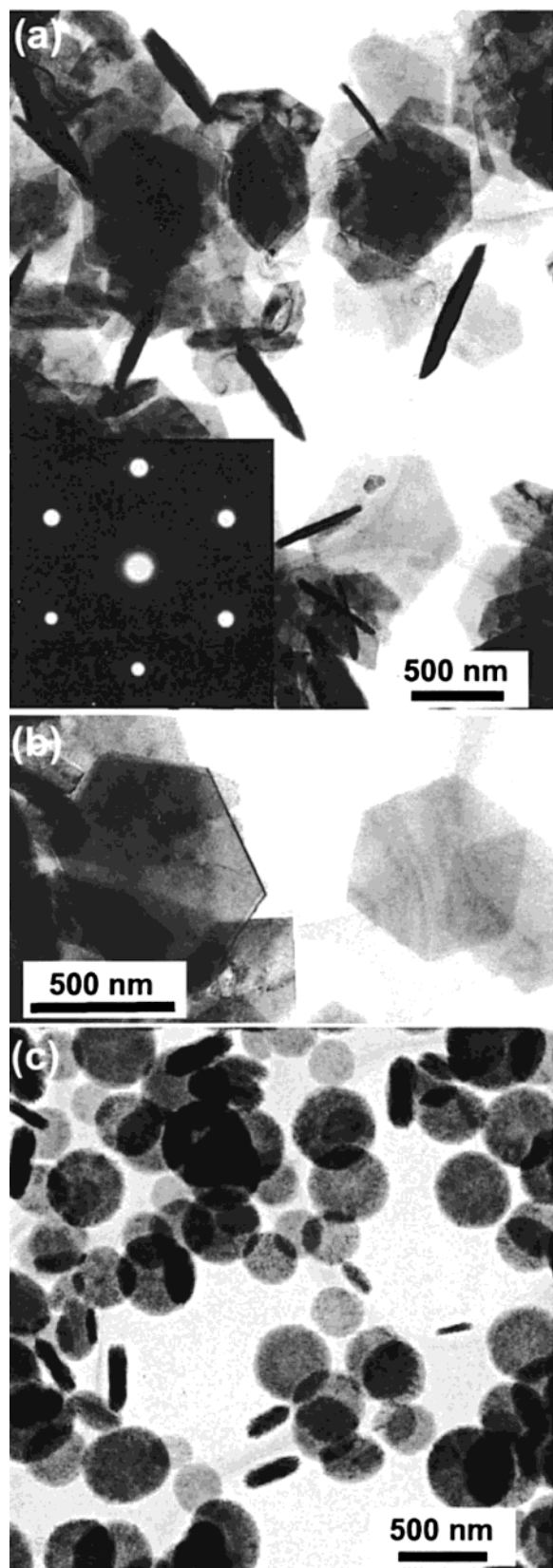(30) Sapieszko, R. S.; Matijevic, E. *J. Colloid Interface Sci.* **1980**, *74*, 405.

Figure 6. TEM images of the product obtained after hydrolysis in the presence of additives and subsequent hydrothermal treatment at 150 °C for 3 days. (a), (b) Surveys of the product obtained in the presence of hydrazine comprising single crystals with a hexagonal morphology. The inset shows the electron diffraction pattern. (c) Survey of hematite particles obtained after addition of acetyl acetone.

thickness of ≈50 nm. The size distribution is broad, but the thickness is always relatively small. This points to a quite selective blocking of the crystal faces by the hydrazine, thus, stimulating a growth in the plane directions. In addition, these platelets are microscopic single crystals (Figure 6b), as can be seen from electron diffraction measurements (Figure 6a, inset) and TEM investigations of particles that are oriented in an upright position (Figure 6a). XRD measurements (data not shown) exhibit sharp lines, indicating that the single-crystalline domains are fairly large. The powder pattern corresponds to hematite with all reflections of the same peak width. That means that the addition of hydrazine changes the particle shape but not the oxidation state of the iron. α-Fe_2O_3 crystals with a hexagonal shape were already found before by aging of ferric salt solutions in the presence of EDTA and KNO_3.[20] However, these platelike particles were much larger, with diameters ranging from 5 to 6 μm and a thickness of about 200 nm.

The addition of acetyl acetone during the synthesis procedure also has some interesting effects. The hematite particles keep their disclike shape similar to the product obtained without any additives, but the particle size is much smaller. The diameters range from about 0.25 to 0.45 μm with a relatively wide size distribution (Figure 6c). The particles are about 80-nm thick and thus are much thinner than the product obtained without any additives. This result suggests that the addition of acetyl acetone obviously enhances the nucleation rate. Because the addition of hydrazine and acetyl acetone during the synthesis has a considerable effect on the size and shape of the iron oxide particles, the tailoring of the material morphology is possible to a certain extent.

Conclusion

Disclike hematite particles with a narrow size distribution were synthesized in good yield using an iron–polyolate complex. With this approach, a novel and comfortable route to iron oxide colloids is available in addition to the well-known inorganic salt routes. Because of its easy synthesis and air stability, this precursor provides an advantageous and cheap access to iron oxide colloids in gram quantities. Without the use of additional templates, the formation of the colloidal material is highly regulated, leading to monodispersed particles with a well-defined morphology. This is probably due to the structure-directing effect of the hydrolyzed polyalcohol ligand. The presented *Fe₆-method* is less sensitive to variations of the reaction parameters than the forced hydrolysis of iron salts and, thus, can easily be reproduced and scaled-up. Furthermore, the addition of hydrazine or acetyl acetone opens the possibility to vary the particle size and shape. But regardless of the morphology, all particles are hematite at the end of the reaction.